Electronic Supplementary Information (ESI) for Analyst

This journal is © The Royal Society of Chemistry 2015

Electronic Supplementary Information

Deformability and size-based cancer cell separation using an integrated microfluidic device

Long Pang,[a] Shaofei Shen,[a] Chao Ma,[a] Tongtong Ma,[a] Rui Zhang,[b] Chang Tian,[a] Lei Zhao,[a] Wenming Liu,[a] and Jinyi Wang*[a]

[a]*Colleges of Veterinary Medicine and Science, Northwest A&F University, Yangling, Shaanxi 712100, China*

[b]*Department of Biochemistry & Biophysics, Texas A&M University College Station, TX 77843, USA*

Abstract. This supplementary information provides all the additional information as mentioned in the text.

Materials and reagents

RTV 615 poly(dimethylsiloxane) (PDMS) pre-polymer and curing agent were purchased from Momentive Performance Materials (Waterford, NY, USA); surface-oxidized silicon wafers were from Shanghai Xiangjing Electronic Technology, Ltd. (Shanghai, China); AZ 50XT photoresist and developer were from AZ Electronic Materials (Somerville, NJ, USA); acridine orange (AO), propidiumiodide (PI) and poly-lysine were from Sigma–Aldrich (MO, USA); polystyrene microspheres (10.5 μm in diameter) fluorescently labeled with dragon green (FS07F) were from Bangs Laboratories, Inc.; cell culture medium, fetal bovine serum (FBS), CellTracker Green CMFDA and CellTracker Orange CMRA were from Gibco Invitrogen Corporation (CA, USA). The analytical reagent-grade solvents and other chemicals were purchased from local commercial suppliers, unless otherwise stated. All solutions were prepared using ultra-purified water supplied by a Milli-Q system (Millipore®).

Device fabrication

The microfluidic device utilized for this study was fabricated using a multilayer soft lithography method.[1] Two different molds were first produced by photolithographic processes to create the fluidic components (channel width: 200 μm, height: 25 μm; cell separation chamber width: 1 500 μm, height: 25 μm, length: 7,000 μm; filter unit height: 25 μm, the pore width: 20, 18, 16, 14, 12, 10, 8 or 6 μm, respectively.) and control channels (width: 100 to 200 μm; height: 25 μm) embedded in the respective layers of the PDMS. To prepare the mold utilized for the fabrication of the fluidic components, a 25 μm thick positive photoresist (AZ 50XT, AZ Electronic Materials) was spin-coated onto a silicon wafer. After UV exposure, the fluidic components on the wafer were developed using an AZ 400K developer (AZ Electronic Materials). The mold for the control channels was made by introducing a 25 μm thick negative photoresist (SU8-2025, Micro.Chem) pattern on a silicon wafer. To achieve reliable performance of each valve, the widths of the control channels were set to 200 μm wide in the sections where the valve modules were located.

Before fabricating the microfluidic device, both the fluidic and control molds were exposed to trimethylchlorosilane (TMSCl) vapor for 2–3 min.[2] A well-mixed PDMS pre-polymer (RTV

615 A and B in 5 to 1 ratio) was poured onto the fluidic mold placed in a Petri dish to yield a 3 mm thick fluidic layer. Another portion of PDMS pre-polymer (RTV 615 A and B in 20 to 1 ratio) was spin-coated onto the control mold (1600 rpm, 60 s, ramp 15 s) to obtain the thin control layer. The thick fluidic layer and thin control layer were cured in an 80 ^{o}C oven for 50 min. After incubation, the thick fluidic layer was peeled off the mold, and holes were introduced into the fluidic layer for cell and nutrient supply access, chamber purging, and waste exclusion. The fluidic layer was then trimmed, cleaned, and aligned onto the thin control layer. After baking at 80 ^{o}C for 60 min, the assembled layers were peeled off the control mold, and another set of holes was punched for access of control channels. These assembled layers were then placed on top of a glass slide coated (3000 rpm, 60 s, ramp 15 s) with PDMS pre-polymer (GE RTV 615 A and B in 10 to 1 ratio) that had been cured for 15 min in the oven (80 ^{o}C). The microfluidic device was ready for use after baking at 80 ^{o}C for 48 h.

Control interface

The control setup consisted of eight sets of eight-channel manifolds (Ningbo Lida Pneumatic Co., Ltd., Ningbo, China) controlled through a NI-PCI-6513 controller board (National Instruments, Austin, TX, USA) connected to a computer through a USB port. Nitrogen gas provided pressure (20 psi) to the manifolds. Twenty-two control channels in the microfluidic device were first filled with water and were individually connected to the corresponding channels on the manifolds with metal pins (23 Gauge, Jinke Wei Corp, China) using polyethylene microbore tubing. When a regulator on the manifold was activated, nitrogen gas entered the respective control line connected with the regulator, providing pressure to closed valves in the microfluidic device. The control interface was created using LabVIEW program (Version 8.0, National Instrument Inc.) on a personal computer, allowing for manual control of individual valves and automation of the microfluidic system.

Cell size measurements

Before the separation experiments, the size of the cancer cell lines was measured.[3] Specially,

the cancer cells were collected after growing in serum-free medium (DMEM supplemented without FBS) for 48 h. The cells were collected by centrifugation at 200×g for 5 min after washing twice with PBS and treating with trypsin for 10 min. The cell numbers were counted using a hemocytometer under an optic microscope and then cell suspension (in PBS) was serially diluted to 1×10^4 cells/mL with PBS. The diameter of the cancer cells, determined using Image-Pro® Plus 6.0 (Media Cyternetics, Silver Spring, MD) and SPSS 12.0 (SPSS Inc.) software, was an average value obtained from images of 200 suspended cells.

Sample preparation

For the separation of cell mixtures, three types of cells (MCF-7, MDA-MB-231 and MDA231-LM2) and microspheres were used to preliminary evaluate the capability of the device to separate cells with different deformability. MCF-7 cells (stained with green fluorescence) and MDA-MB-231/MDA231-LM2 cells (stained with red fluorescence) were cultured separately. Then, the cancer cells were resuspended in the buffer (PBS, 0.01 mol/L, PH 7.4; citric acid, 4.8 g/L; trisodium citrate, 13.2 g/L; and dextrose, 14.7 g/L) with 1% bovine serum albumin (Invitrogen) at a concentration of 1×10^6 cells/mL.[2] The suspension of the fluorescent microspheres (1×10^6 microspheres/mL) was prepared by diluting the microspheres in ultra-purified water containing 0.5% w/v Tween 20. Prior to each experiment, the microsphere suspension in a 15 mL vial was sonicated for at least 8 min to achieve a sufficiently mono-dispersed suspension.[4]

Two types of cell mixtures (MCF-7 and MDA-MB-231 cells, and MCF-7 and MDA231-LM2 cells) were used to evaluate the ability of the device to separate cells from a cell mixture. Specially, MCF-7 cells (stained with green fluorescence) and MDA-MB-231 or MDA231-LM2 cells (stained with red fluorescence) were cultured separately. Then, MCF-7 and MDA-MB-231 (or MDA231-LM2) cells were mixed in equal amounts with a final density of 1×10^6 cells/mL. The mixture of MCF-7 and MDA-MB-231 (or MDA231-LM2) cells contained 5×10^5 cells/mL for each cell line.

For the separation of cancer cells from blood samples, the whole blood samples were obtained from healthy volunteers and collected in ethylenediaminetetraacetic acid vacuum

tubes. Prior to use, the samples were diluted to 1:4 (v:v) with the buffer (PBS, 0.01 mol/L, PH 7.4; citric acid, 4.8 g/L; trisodium citrate, 13.2 g/L; and dextrose, 14.7 g/L),corresponding to a hematocrit of 8% and the density of erythrocytes was 1×10^9 cells/mL. All the blood samples were used within 6 h after collection. The suspensions of MCF-7 cells (stained with green fluorescence) and MDA-MB-231/MDA231-LM2 cells (stained with red fluorescence) with the cell density of 1×10^6 cells/mL were prepared by resuspended in the buffer supplemented with 1% bovine serum albumin.

To evaluate the collection efficiency of blood cells and cancer cells, the cancer cell suspension were diluted to the cell density of 1×10^3 cells/mL using the previous method.[4] Then, the cancer cell suspension (1×10^3 cells/mL) or diluted blood (1×10^9 erythrocyte/mL) was separately infused into the device.

To carry out the separation of cancer cells from the whole blood, mimicking the isolation of rare cells from human peripheral blood, the fluorescence labeled cancer cells MCF-7, MDA-MB-231 or MDA231-LM2 (~1×10^4 cells) were mixed separately with diluted whole blood (~10 mL) at a final cancer cell-to-blood cell ratio of $1/10^6$. In detail, 2 mL whole human blood were combined with 0.01 mL cancer cells (1×10^6 cells/mL). Then, the mixture was diluted with 8 mL buffer (PBS, 0.01 mol/L, PH 7.4; citric acid, 4.8 g/L; trisodium citrate, 13.2 g/L; and dextrose, 14.7 g/L).

Numerical simulations

To evaluate velocity field fluctuations in the device, computational fluid dynamics (CFD) simulation was performed using ESI-CFD software (V2010.0, ESI CFD, Inc.). The simulation environment was verified for steady incompressible flows. Constant flow rate were specified at the input, and the outlet was set to a fixed-pressure boundary condition. No slip boundary condition was applied at the channel walls. FLOW module in CFD-ACE+ were used to explore the flow velocity distribution in the microchannels. Based on the finite volume method, the conservation of Navier–Stokes momentum in the device is described by the equation (Eq. S1) as follows.[2]

$$\frac{\partial}{\partial t}(\rho\vec{V}) + \nabla(\rho\vec{V}\vec{V}) = -\nabla P + \nabla\bar{\bar{\tau}} \quad \text{(Eq. S1)}$$

The conservation of mass is described by the continuity equation (Eq. S2) as follows.

$$\frac{\partial \rho}{\partial t} + \nabla(\rho \vec{V}) = 0 \qquad \text{(Eq. S2)}$$

where ρ is the fluid density, $\vec{V}$ is the velocity vector of the fluid, P is the pressure and $\bar{\bar{\tau}}$ is the stress tensor.

Collection efficiency and purity

For the studies of single cell line distribution and the separation of cell mixtures, the collection efficiency of cells was calculated using the following equation (Eq. S3).

$$Collection\ efficiency = \frac{Cancer\ Cell_{outlet}}{Cancer\ Cell_{inlet}} \times 100\% \qquad \text{(Eq. S3)}$$

Where $Cancer\ Cell_{outlet}$ is the cells collected from the cell outlet, $Cancer\ Cell_{inlet}$ is the cells infused into the device from the cell inlet.

The purity of the recovered cells from the mixtures of two types of cells was calculated using the following equation (Eq. S4).

$$Purity = \frac{Target\ CancerCell_{outlet}}{Total\ CancerCell} \times 100\% \qquad \text{(Eq. S4)}$$

Where $Target\ Cancer\ Cell_{outlet}$ is the target cells collected from the cell outlet of 20-12 μm or 10-6 μm filter matrices, $Total\ Cancer\ Cell$ is the whole cells collected the cell outlet of 20-12 μm or 10-6 μm filter matrices.

For the separation of cancer cells from blood samples, the collection efficiency and purity of the recovered cancer cells were calculated using the following equations (Eq. S5 and Eq. S6).

$$Collection\ efficiency = \frac{m_{outlet} W_{outlet}}{m_{inlet} W_{inlet}} \times 100\% \qquad \text{(Eq. S5)}$$

$$Purity = \frac{m_{outlet} W_{outlet}}{m_{outlet} W_{outlet} + m_{outlet}} \times 100\% \quad \text{(Eq. S6)}$$

Where m_{outlet} is the number of blood cells collected from the cell outlet, m_{inlet} is the number of blood cells in the original sample, W_{outlet} is the ratio of cancer cells to blood cells in all the cells collected from the cell outlet, W_{inlet} is the ratio of cancer cells to blood cells in the original sample.

To further evaluate the purity of the recovered cancer cells, we also divided the recovered cells into two parts according to the pore size of the filter matrices (20-12 μm and 10-6 μm). In this study, the purity of cells was calculated using the following equation (Eq. S7).

$$Purity = \frac{V_{outlet1}}{V_{outlet1} + n_{outlet1}} \times 100\% \quad \text{(Eq. S7)}$$

Where $n_{outlet1}$ is the number of blood cells collected from 20-12 μm or 10-6 μm filter matrices, $V_{outlet1}$ is the cancer cells collected from the outlets of 20-12 μm or 10-6 μm filter matrices.

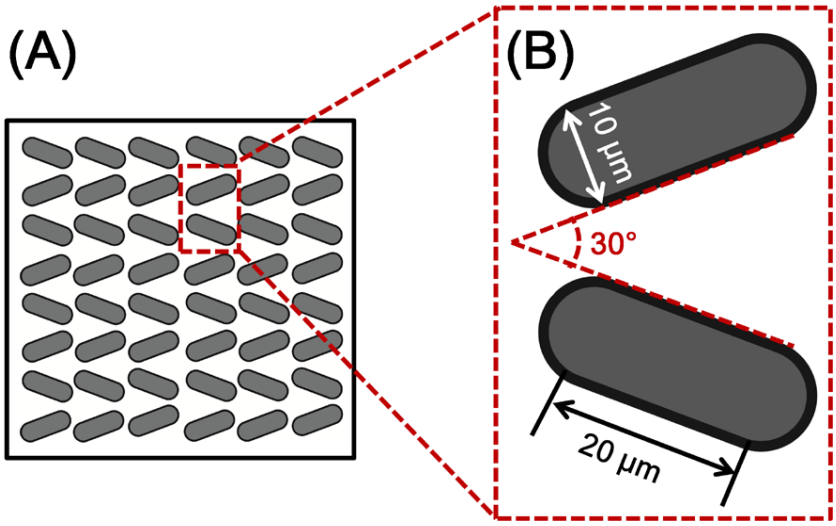

Fig. S1. (A) Schematic diagram of the typical funnel-like filter matrix. Each funnel-like filter matrix was composed of 6 columns and many rows. (B) Schematic diagram of one funnel-like filter unit, which was enlarged to view the dimensions. The filter unit consisted of two semicircles (the diameter is 10 μm) and a rectangle (the length is 20 μm and width is 10 μm).

Two neighboring filter units formed a funnel-like architecture with a minimum cross-sectional area (30^{o}) for cell capture.

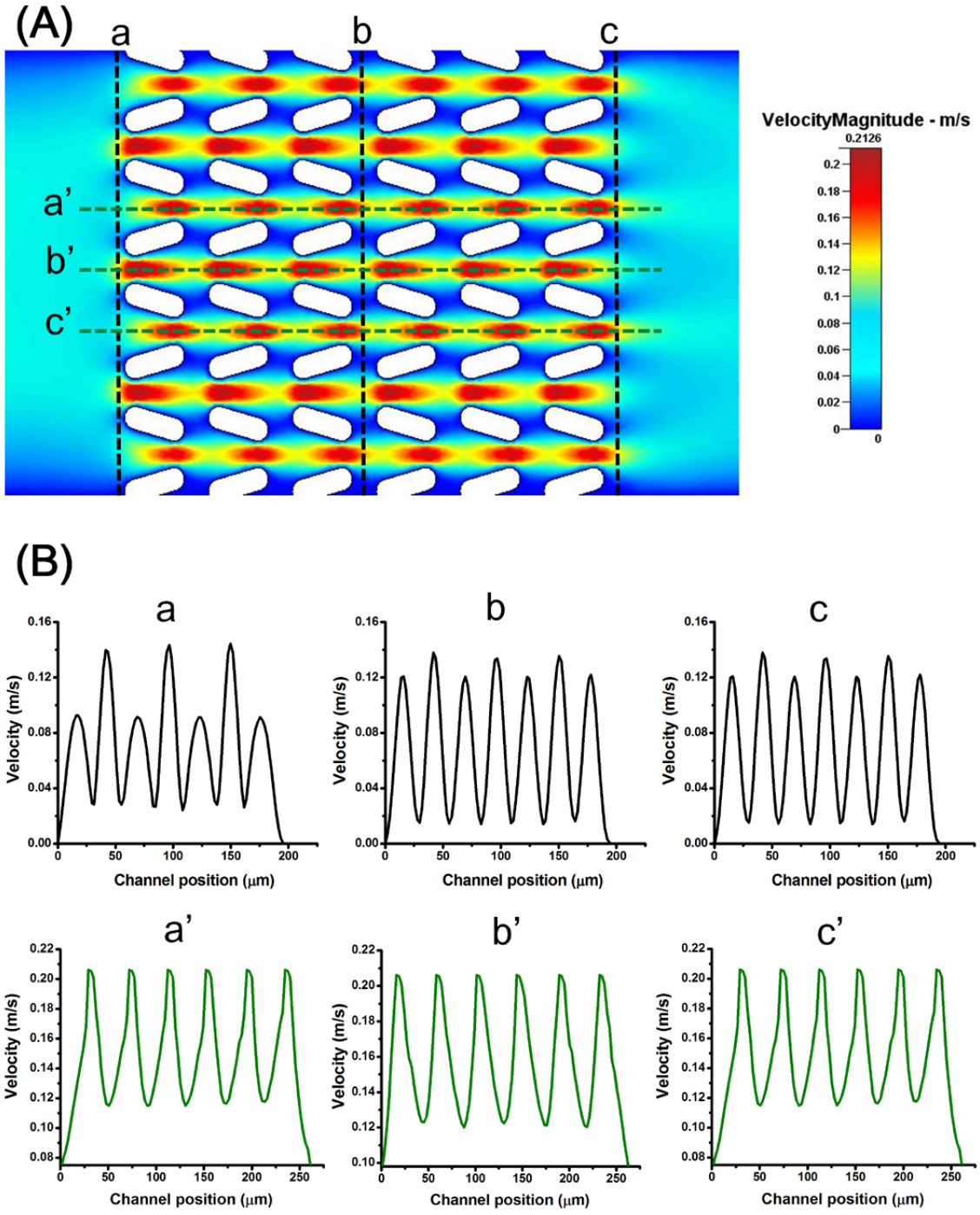

Fig. S2. Computational simulation of the fluid velocities in 10-μm filter matrix (the pore size is 10 μm) at a flow rate of 203 μL/min (the velocity magnitude is 0.067 m/s). (A) Fluid velocity pattern formed in the 10-μmfilter matrix. The black and green dotted lines (a, b, c, a', b' and c') were used to analyze the fluid velocity distributions in the 10-μm filter matrix. (B) Quantitative

comparison of the fluid velocities in the 10-μm filter matrix under the flow rate of 203 μL/min, respectively corresponding to the positions of the black and green dotted lines (a, b, c, a', b' and c') in (A).

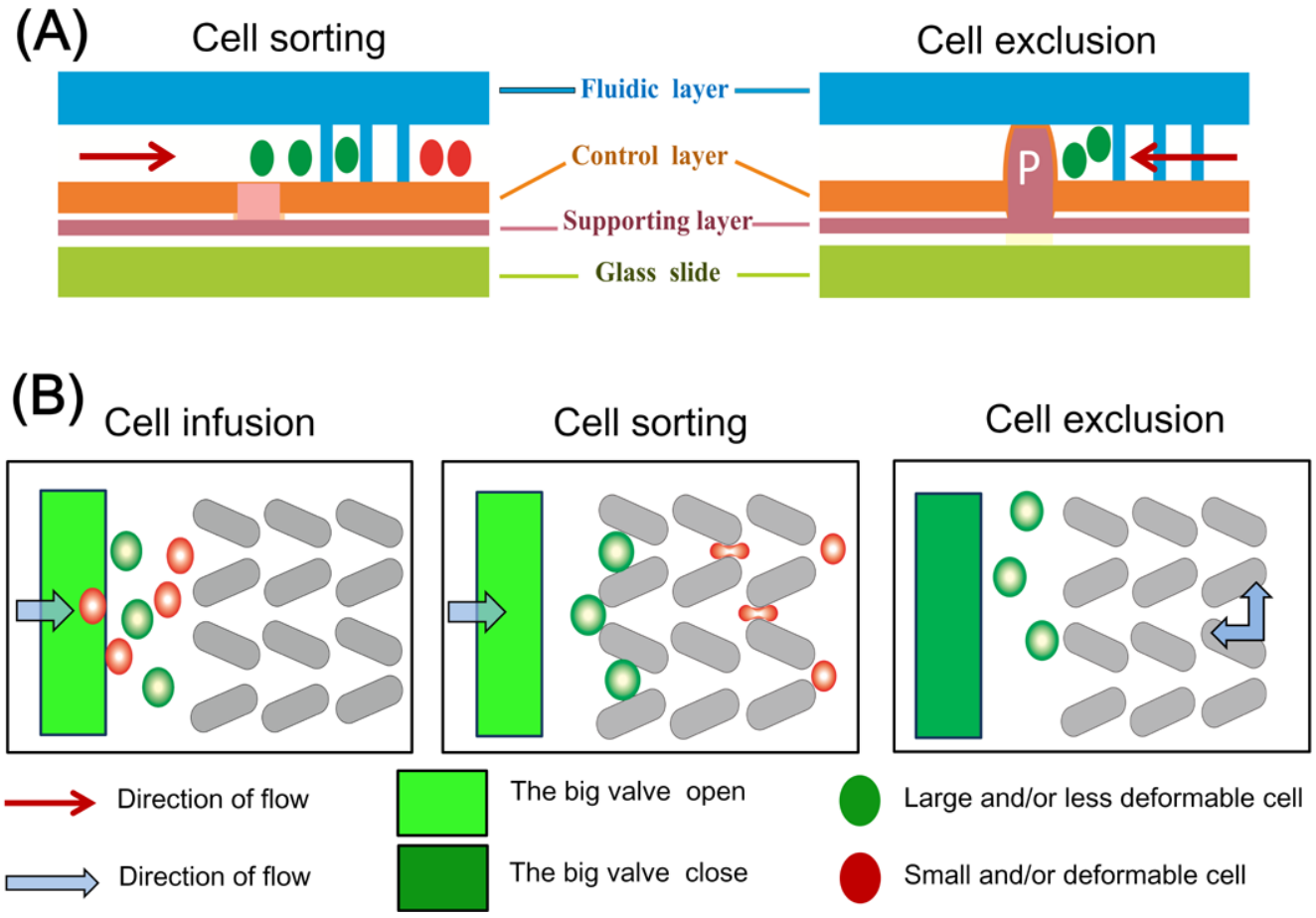

Fig. S3. (A) The lateral view schematic diagram of cell sorting and exclusion, showing the device had four layers: fluidic layer, control layer, supporting layer and glass layer. (B) Schematic diagrams of the operation of the microvalve located between two adjacent filter matrices during a three-step cycle of infusion, sorting and exclusion. During the cell infusion and sorting, the microvalve was opened to allow the cell sample flow through the filter matrices for cell sorting according to their size and deformability. During the cell exclusion, the microvalve was closed to allow the sorted cells sequentially into their own outlet channel.

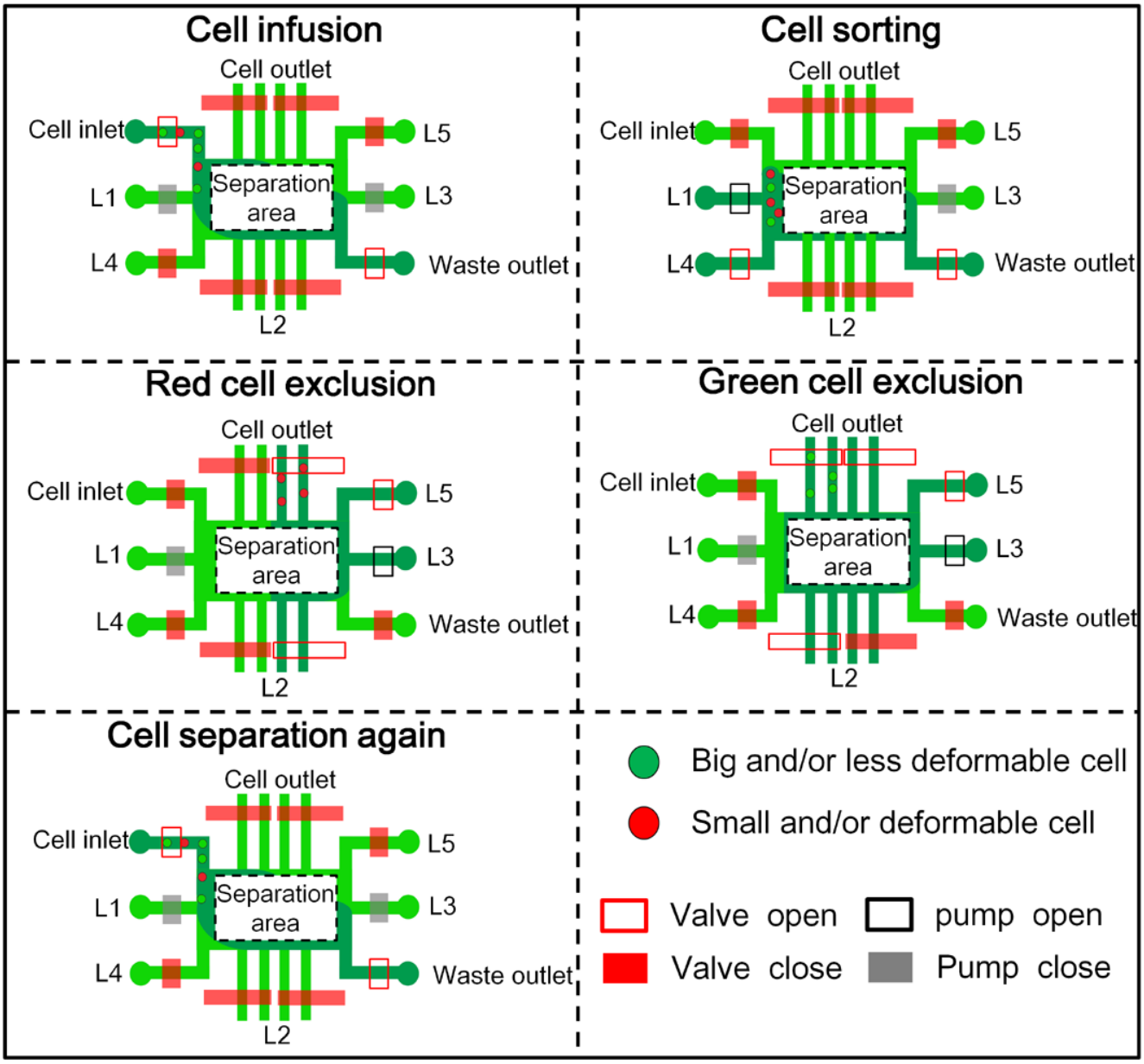

Fig. S4. Schematic diagram of the operation of the cell separation device on a repeating three-step cycle of infusion, sorting and exclusion. Cell sample was delivered from the cell inlet. L1, L2 and L3 channels were used for the buffer infusion, which could drive the cell samples to pass through the filter matrices or the sorted cells to go out the device. The L4 and L5 channels were designed to facilitate the work of L1 and L3 when needed during cell introduction or exclusion. The detailed design on the separation area was shown in Fig.1A, and its operation was shown in Fig.1C. The cell inlet and waste outlet were designed for cell sample introduction and waste exclusion.

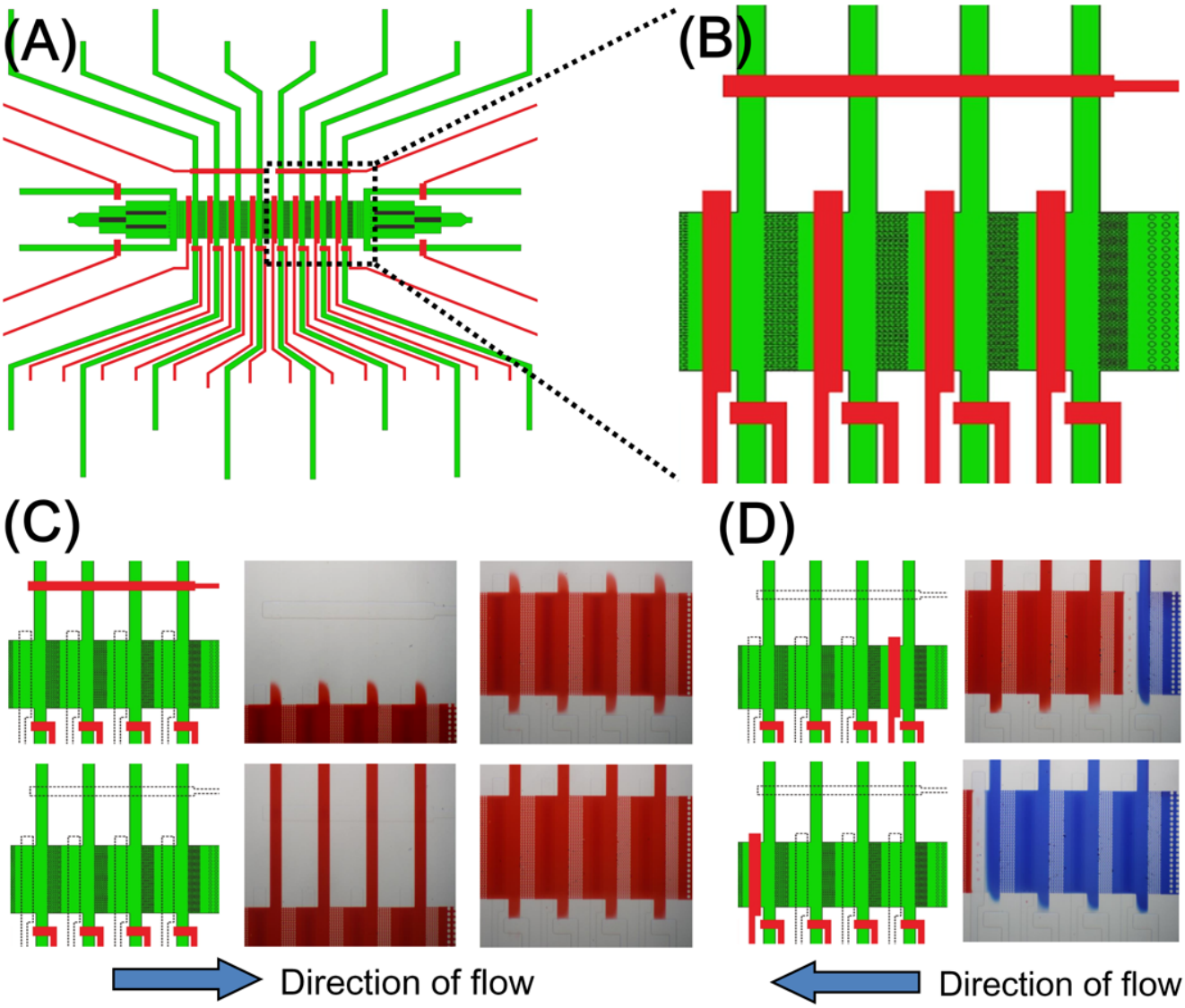

Fig. S5. The infusion of two different food-dye solutions (red and blue for easy visualization) into the device, simulating the cell separation processes. (A) Schematic diagram of the designed microdevice. Green indicates the fluidic channels and red indicates the valves. (B) The enlarged view of the separation area. (C) Infusion of the red flow into the fluidic channels to simulate the cell infusion and sorting steps. On the first row, the cell outlet channels and the L2 buffer infusion channels were all opened by regulating the corresponding valves; On the second row, the L2 buffer infusion channels were still closed, while the cell outlet channels were opened by regulating the corresponding valve. All the valves located between the two adjacent filter matrices were closed to allow the red flow through the filter matrices. The actual views were given, which could be also found in Movie S1. (D) Infusion of the blue flow into the fluidic channels to simulate the cell exclusion step. The food-dye solution was

sequentially pushed out the device under the help of the valves located between the two adjacent filter matrices. On the first row, the first big valve located between 8-μm and 6-μm filter matrices and the corresponding valve (controlling the L2 channel) were opened. On the second row, the last valve located between 14-μm and 12-μm filter matrices and the corresponding valve (controlling the L2 channel) were opened. The actual views were given, which could be also found in Movie S2).

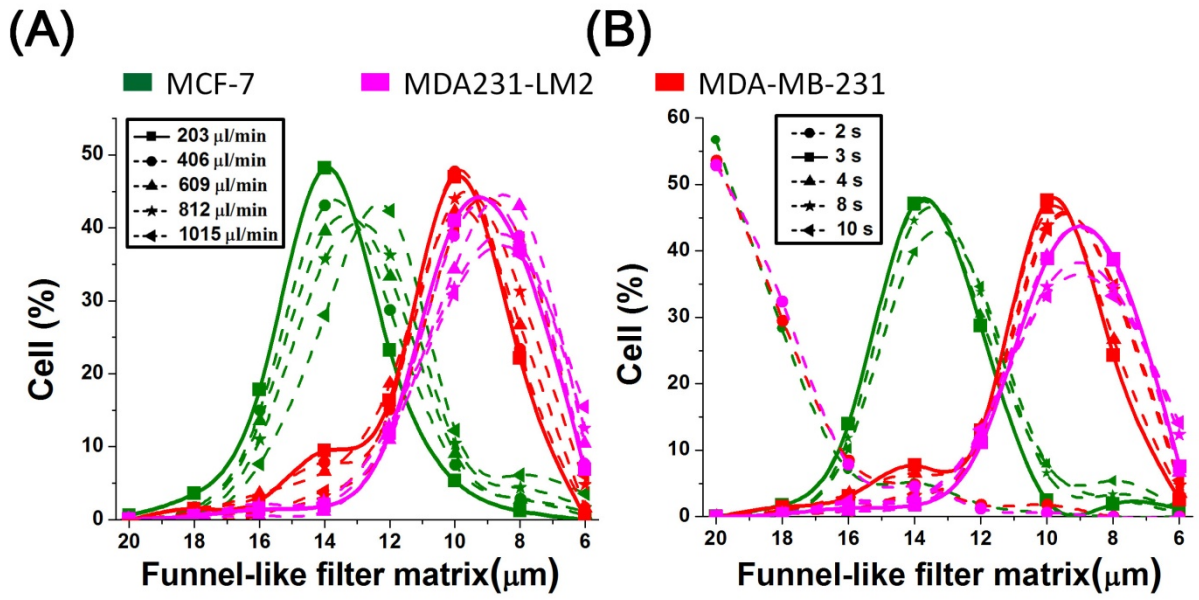

Fig. S6. Optimization of the operating parameters. (A) Effect of the flow rates of the driving buffer infused from L1 channel on the distributions of different cancer cells. Five flow rates (203, 406, 609, 812, and 1015 μL/min) were used in this study. According to Eq.1, these flow rates respectively corresponded to the pressure drop 6, 12, 18, 24, and 32 kPa. (B) Effect of the duration time of the driving buffer infusion on the distributions of different cancer cells. In this study, five duration times (2, 3, 4, 8 and 10 s) were used to optimize the duration time at the driving flow rate of 203 μL/min.

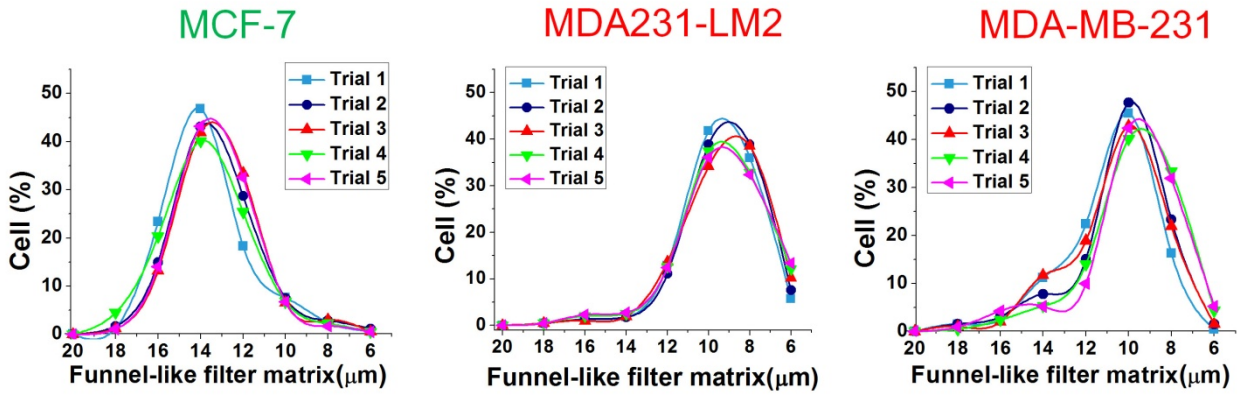

Fig. S7. Repeatability of cancer cell distributions in the filter matrices from 5 separate trials using optimized experimental conditions (the flow rate of the driving buffer was 203 μL/min and the duration time of the driving buffer infusion was 3 s).

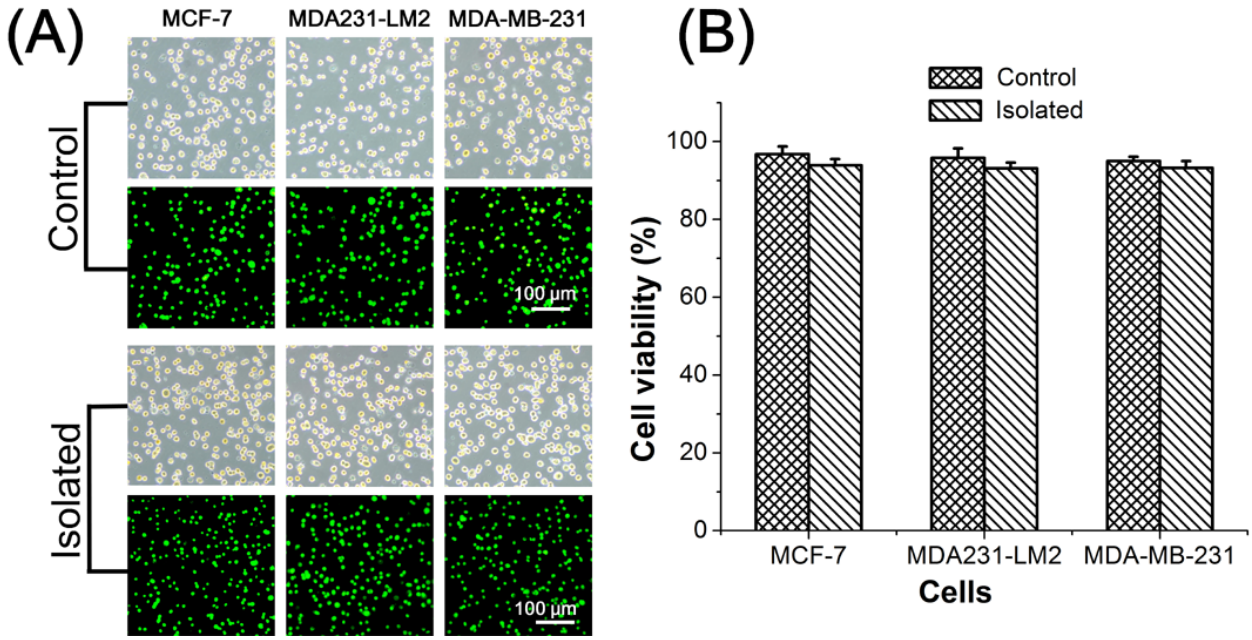

Fig. S8. Comparison of cell viability between the control (unsorted) and sorted cancer cells (MCF-7, MDA231-LM2 and MDA-MB-231 cells) by using AO/PI double-staining protocol. (A) The bright-field (top) and fluorescence (bottom) images of control (rows 1 and 2) and sorted (rows 3 and 4) cells. (B) Quantitative analysis of the cellular viability of the control (unsorted) and sorted cells. The results confirm that cells sorted through the microfluidic system remain highly viable, similar to control cells, retrieving >93% viable cells.

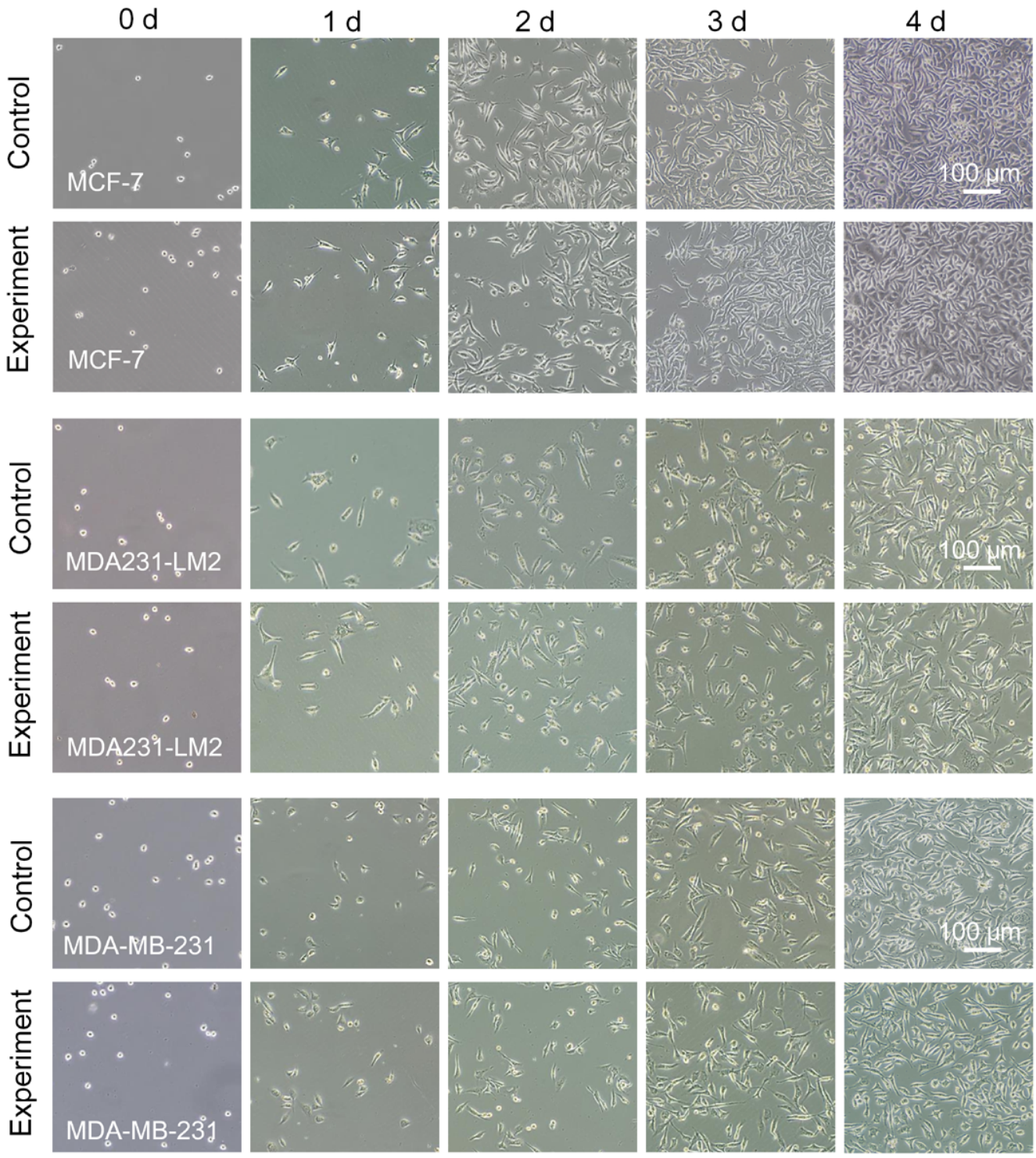

Fig. S9. Viability assays of the sorted cancer cells (MCF-7, MDA231-LM2 and MDA-MB-231 cells) by reseeding cells back into culture. The bright-field images of cultures of control (unsorted) and sorted cells collected from cell outlet of the device. Each type of cancer cells was independently tested under the optimized operation parameters. The cells were reseeded with a density of 1×10^4 cells/mL.

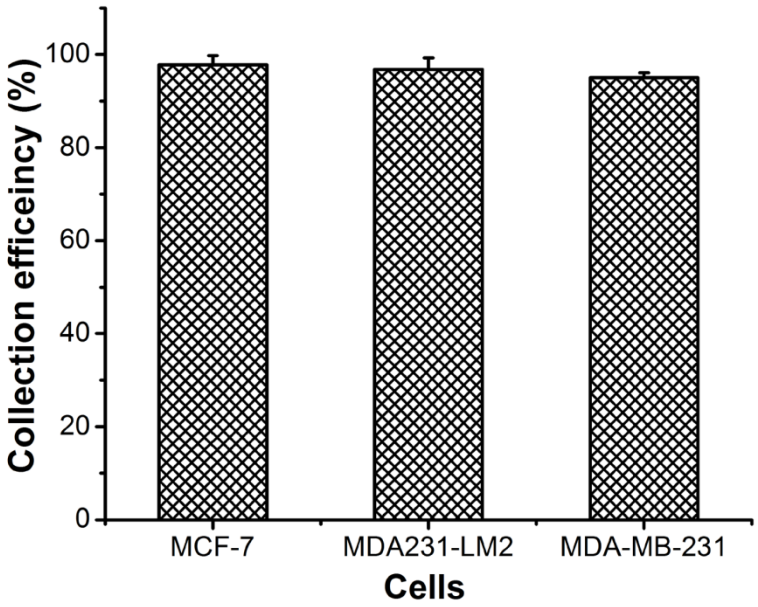

Fig. S10. Statistical results of the collection efficiency by re-collecting the sorted cancer cells (MCF-7, MDA231-LM2 and MDA-MB-231). Each type of cancer cells was independently tested using optimized parameters. Standard deviations deduced from ten parallel experiments were shown as the error bars.

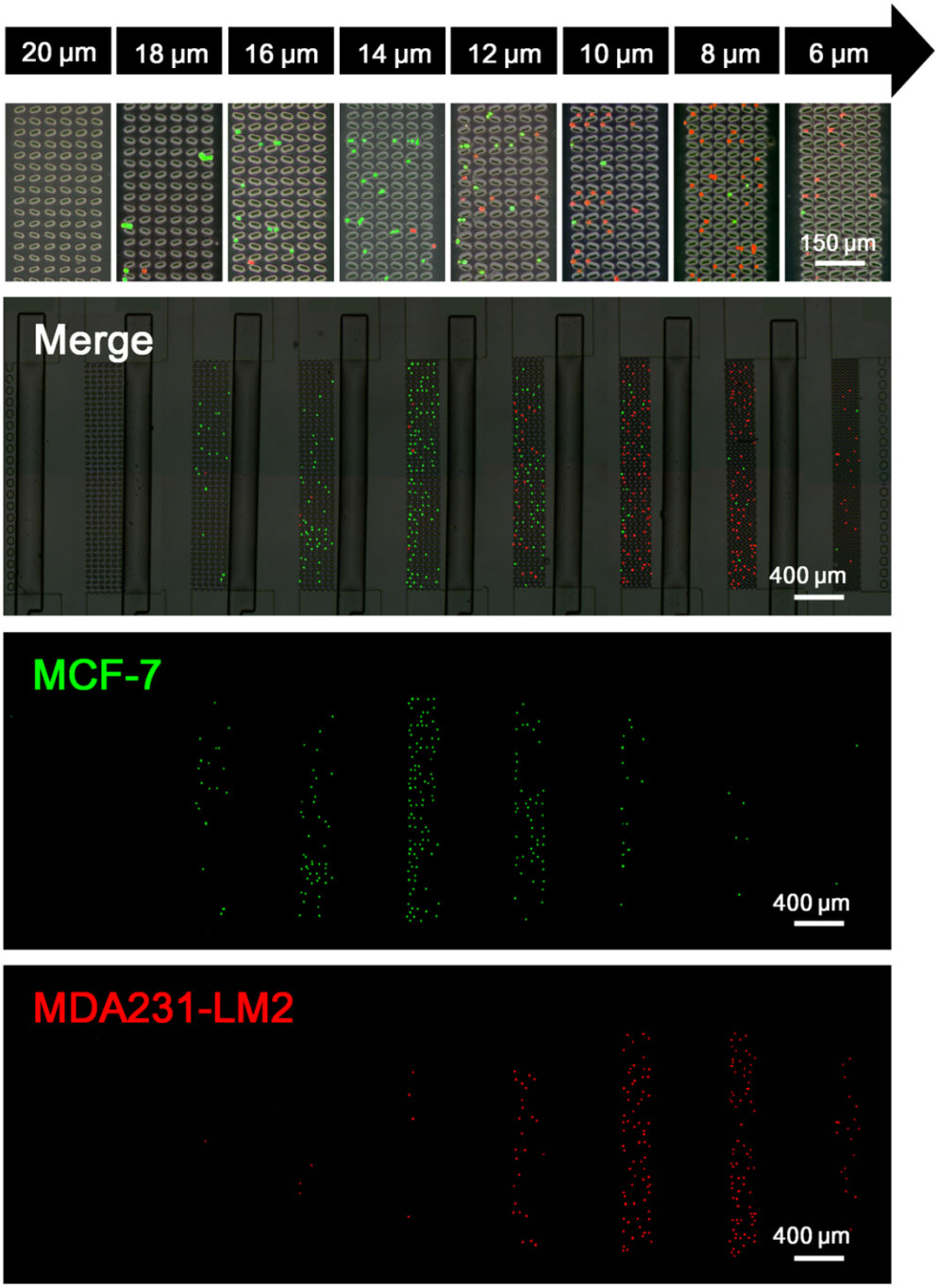

Fig. S11. Fluorescence images of the cells trapped in the filter matrices after the separation of MCF-7 (stained green with Cell Tracker Green CMFDA) and MDA231-LM2 (stained red with Cell Tracker Orange CMRA) cell mixture. Pore sizes were shown in the first row. The second row showed the merged image with a high magnification. Merged, green and red channels were shown in the third to fifth rows to demonstrate cells trapped in filter matrices, indicating the separation efficiency of two types of cells (MCF-7 and MDA231-LM2) through the filter matrices ranging in the pore size from 20 to 6 μm.

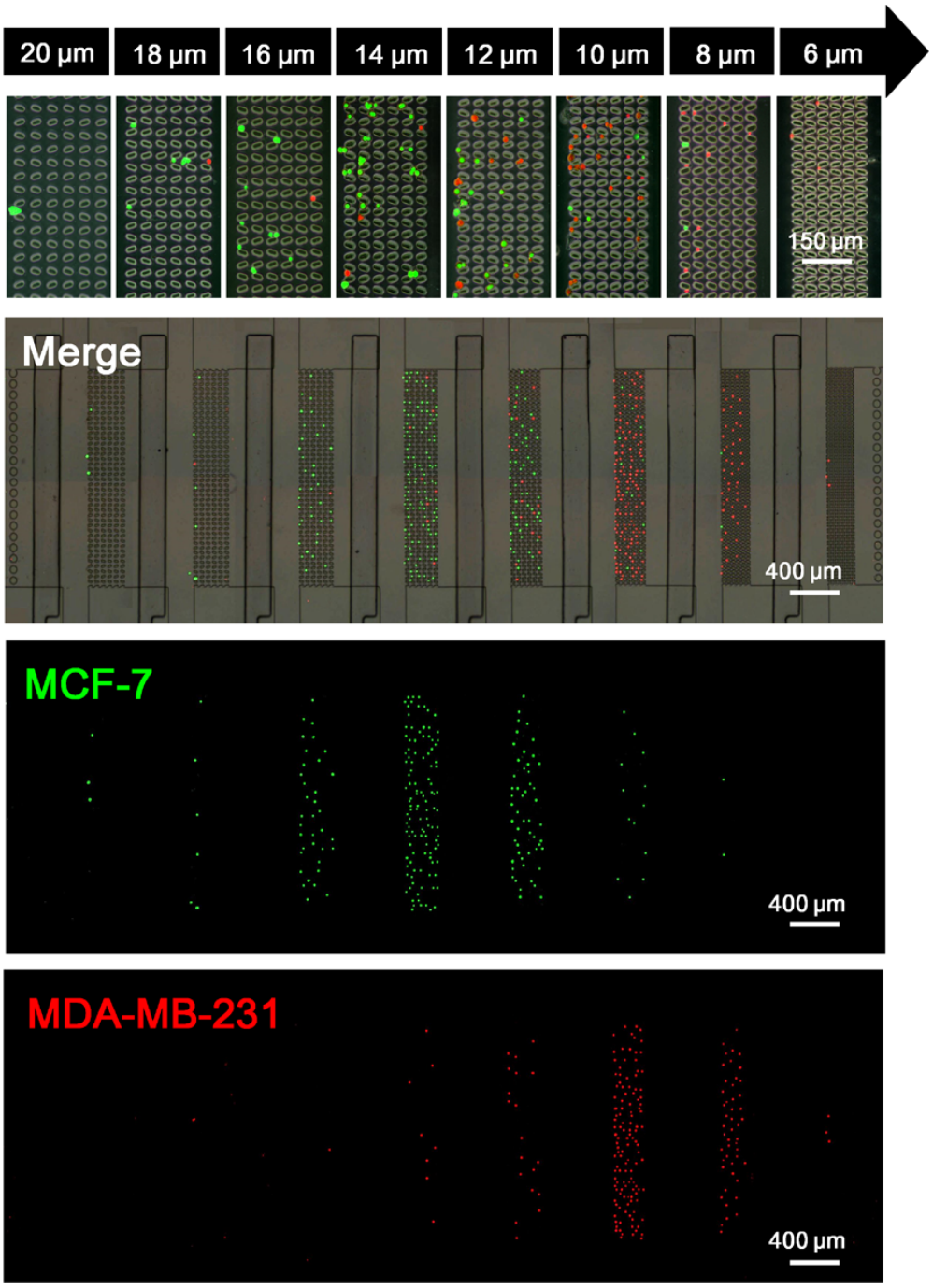

Fig. S12. Fluorescence images of the cells trapped in the filter matrices after the separation of MCF-7 (stained green with Cell Tracker Green CMFDA) and MDA-MB-231 (stained red with Cell Tracker Orange CMRA) cell mixture. Pore sizes were shown in the first row. The second row showed the merged image with a high magnification. Merged, green and red channels were shown in the third to fifth rows to demonstrate cells trapped in filter matrices, indicating the separation efficiency of two types of cells (MCF-7 and MDA-MB-231) through the filter matrices ranging in the pore size from 20 to 6 μm.

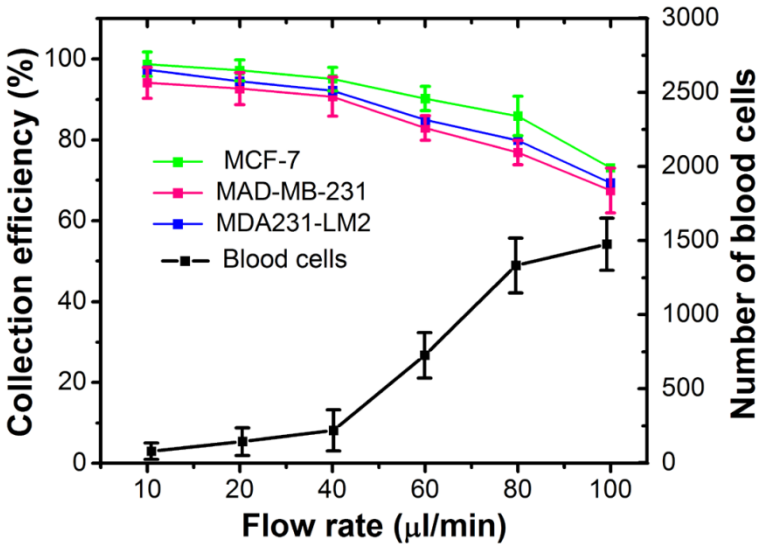

Fig. S13. Plots presenting the effects of the different flow rates of cell sample infusion on the collection efficiency of cancer cells (MCF-7, MDA231-LM2 and MDA-MB-231 cells) and the numbers of trapped blood cells in the filter matrices during the separation of blood samples. Standard deviations deduced from ten parallel experiments were shown as the error bars.

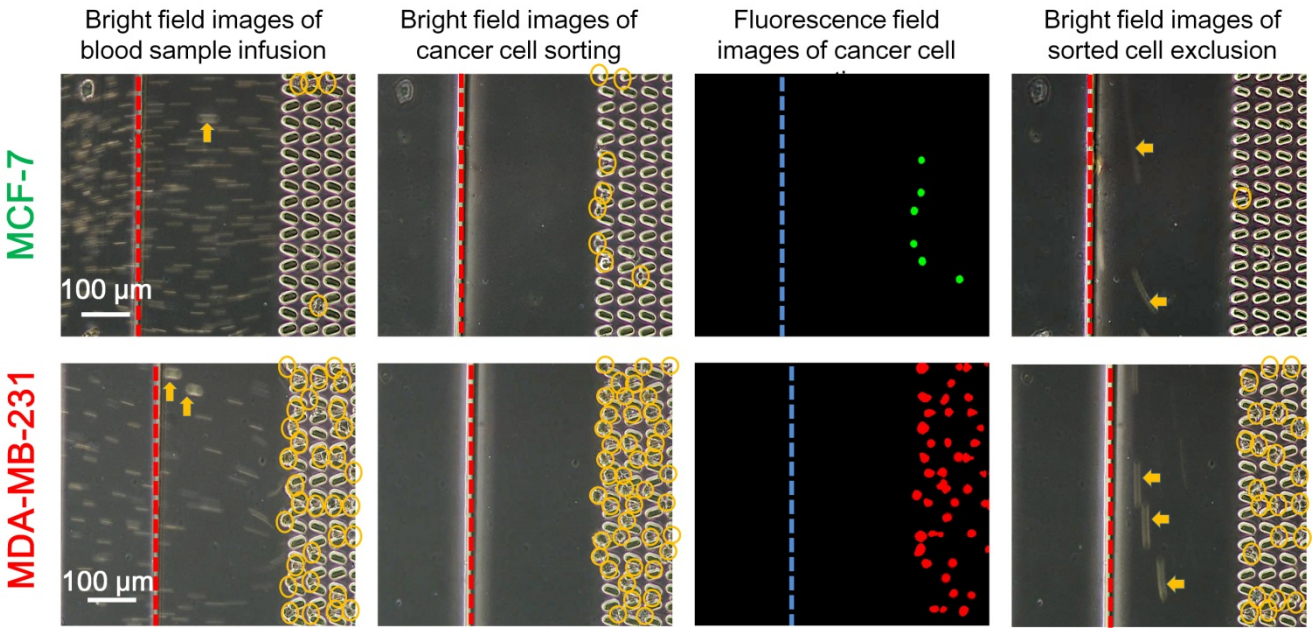

Fig. S14. The typical images of cancer cell-contained blood sample separation during the infusion, sorting and exclusion processes in the 10-μm filter matrix (the pore size is 10 μm). For easily distinguishing from the blood cells, MDA-MB-231 cells were stained red with Cell Tracker Orange CMRA and MCF-7 cells were stained green with Cell Tracker Green CMFDA before the separation experiment. The two types of cancer cells were mixed separately with blood samples at a final cancer cell-to-blood cell ratio of $1/10^6$. The big valve located between the 12-μm and 10-μm filter matrices were on the left (red or blue dotted line).

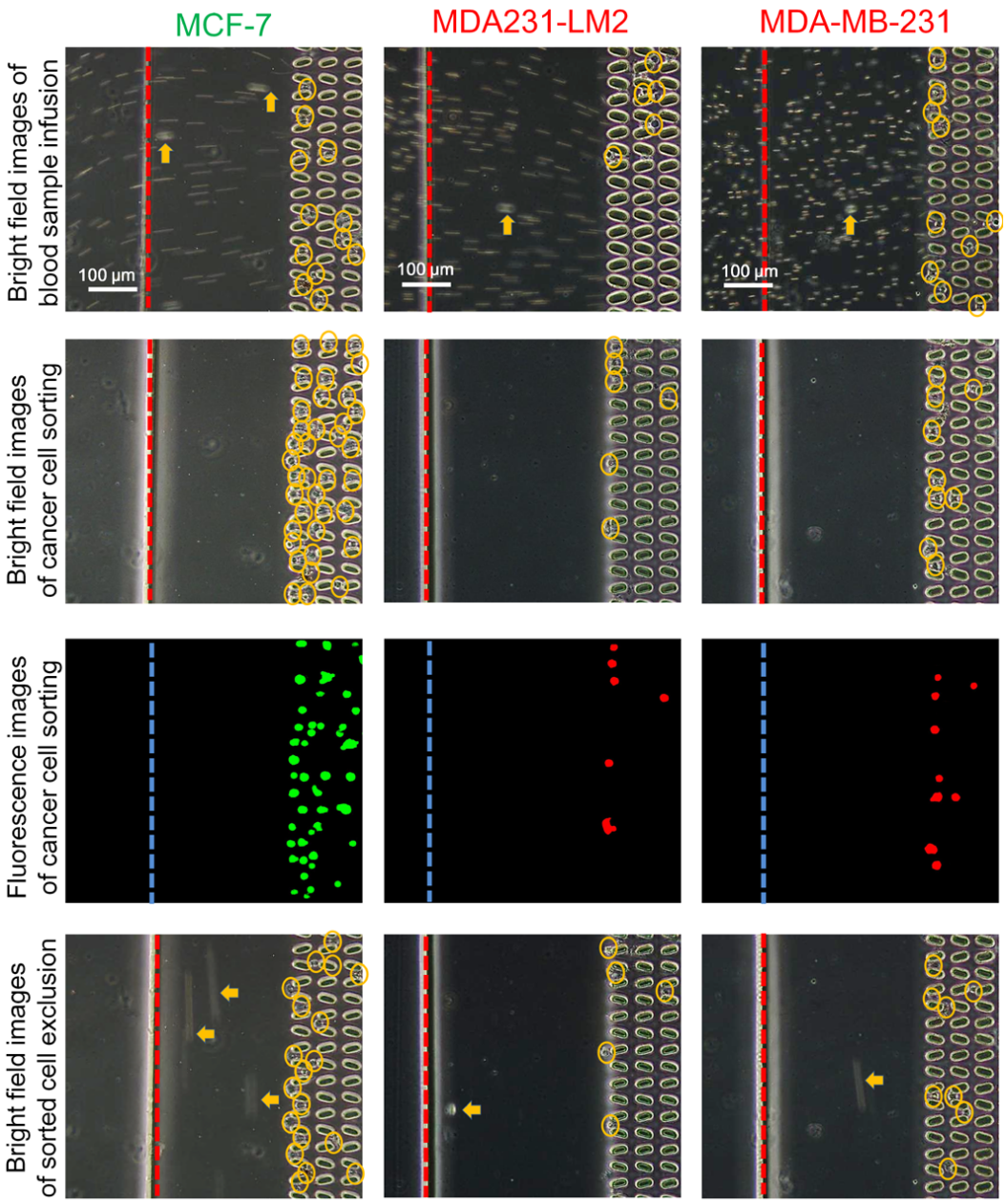

Fig. S15. The typical images of cancer cell-contained blood sample separation during the infusion, sorting and exclusion processes in the 14-μm filter matrix (the pore size is 14 μm). For easily distinguishing from the blood cells, MDA-MB-231 and MDA231-LM2 cells were stained red with Cell Tracker Orange CMRA and MCF-7 cells were stained green with Cell Tracker Green CMFDA before the separation experiment. The three types of cancer cells were mixed separately with blood samples at a final cancer cell-to-blood cell ratio of $1/10^6$. The big valve located between the 16-μm and 14-μm filter matrices were on the left (red or blue dotted line). The separation process of MDA231-LM2 in the 10-μm filter matrix was shown in Movie S5.

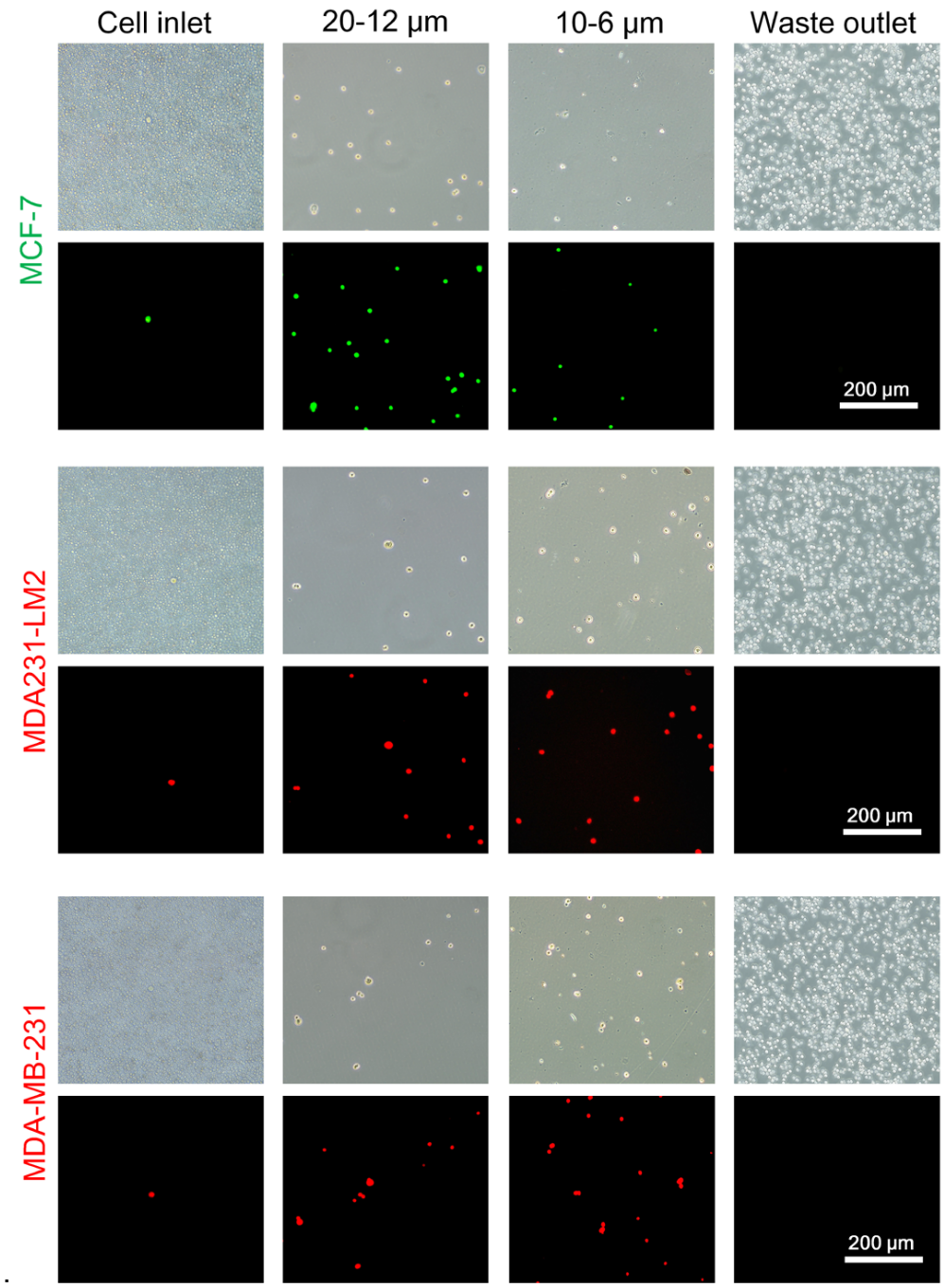

Fig. S16. Representative images of the cancer cells (MCF-7, MDA-MB-231 and MDA231-LM2) collected from the wide (20-12 μm) and narrow (10-6 μm) filter matrices after being separated from the blood samples, which clearly showed the separation efficiency of the microdevice by a comparison of the initial cell sample (Cell inlet) and the cells collected from the waste outlet (Waste outlet). For easily distinguishing from the blood cells, MDA-MB-231 and MDA231-LM2 cells were stained red with Cell Tracker Orange CMRA and MCF-7 cells were stained green with Cell Tracker Green CMFDA.

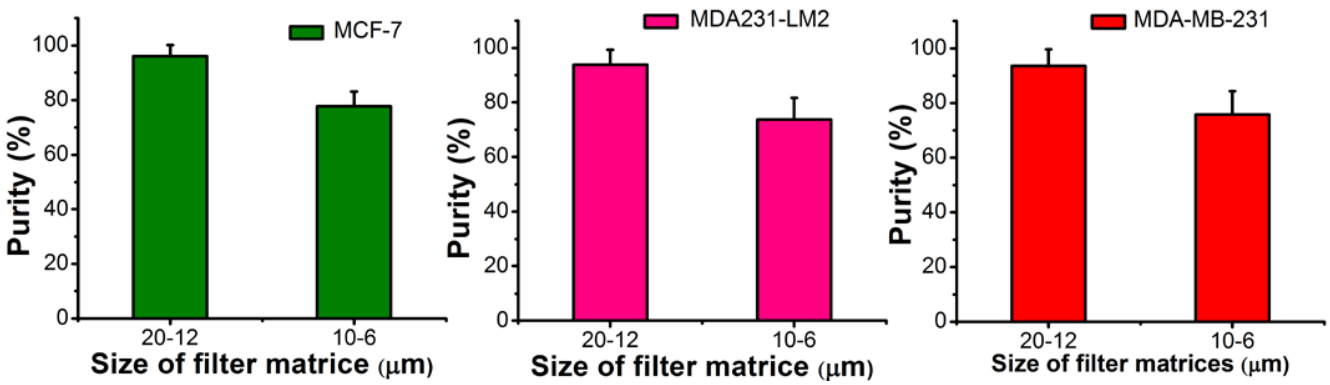

Fig. S17. Quantitative analysis of the purity of the cancer cells (MCF-7, MDA231-LM2 and MDA-MB-231 cells) collected from the wide (20-12 μm) and narrow (10-6 μm) filter matrices after being separated from the blood samples. Standard deviations deduced from ten parallel experiments were shown as the error bars. The results confirm that the purity of the cells collected from the narrow (10-6 μm) filter matrices is less than those from the wide (20-12 μm) filter matrices.

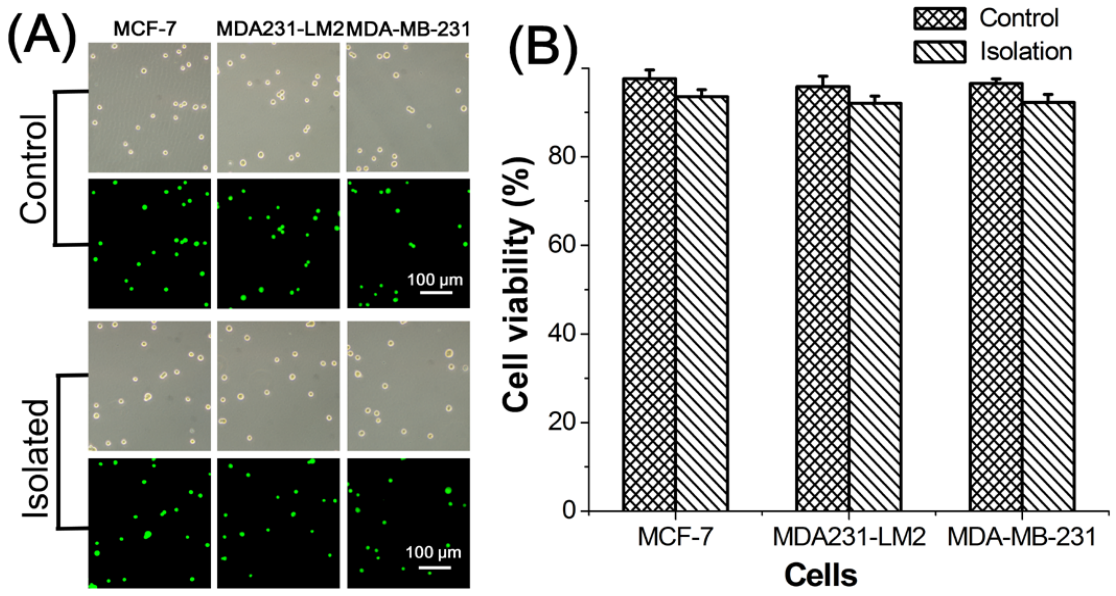

Fig. S18. Comparison of cell viability between the control (unseparated) and separated cancer cells (MCF-7, MDA231-LM2 and MDA-MB-231 cells) by using AO/PI double-staining protocol. (A) The bright-field (top) and fluorescence (bottom) images of the control (rows 1 and 2) and separated (rows 3 and 4) cells. Scale bars, 100 μm. (B) Quantitative analysis of cellular viability of the control (unseparated) and separated cells. The results confirm that cells separated through the microfluidic system remain highly viable, similar to the control cells, retrieving > 92% viable cells.

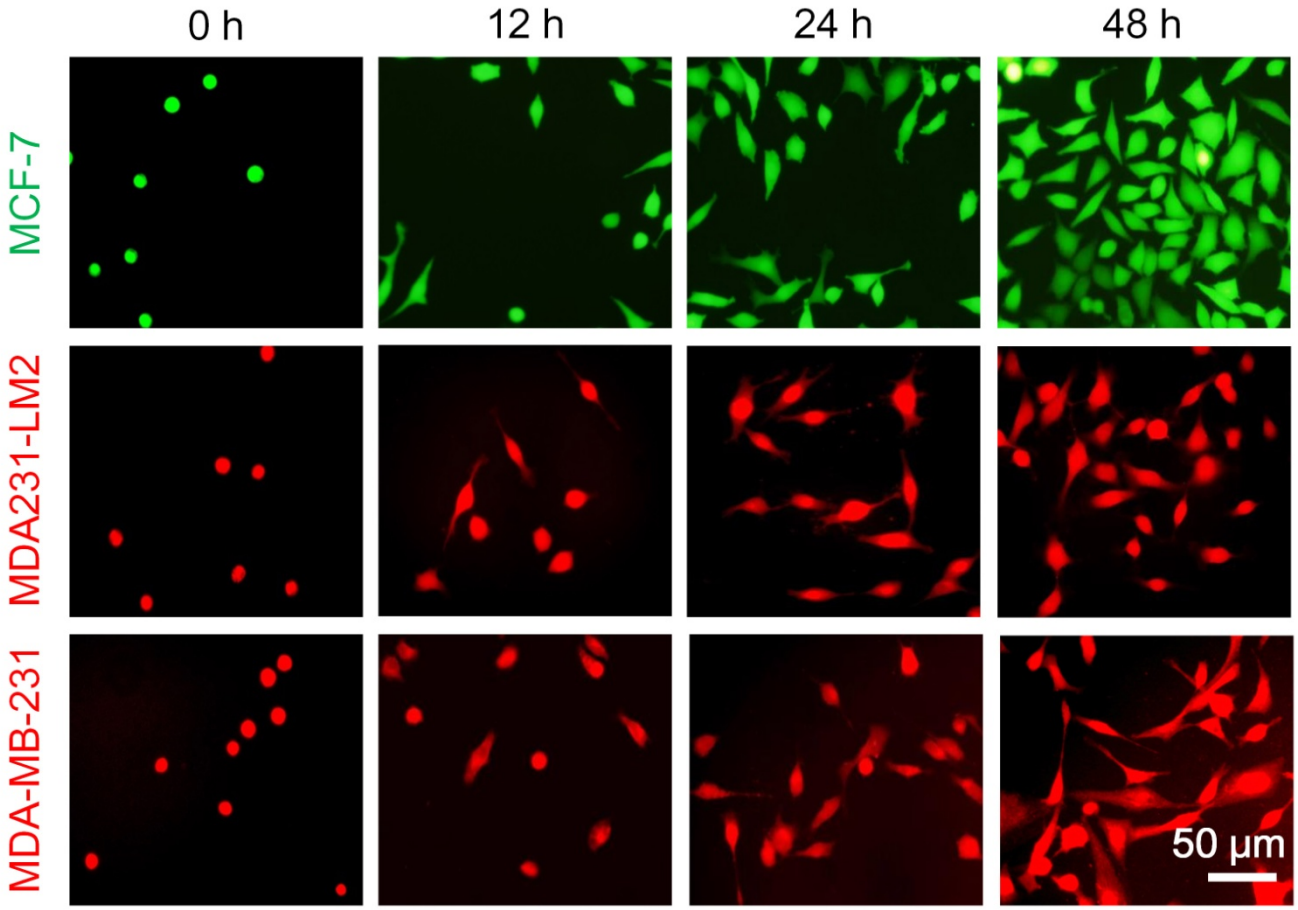

Fig. S19. Cellular viability assay of the three types of cancer cells (MCF-7, MDA-MB-231 and MDA231-LM2 cells) cultured of control (unseparated) cells for 48 h. Before the experiment, MDA-MB-231 and MDA231-LM2 cells were stained red with Cell Tracker Orange CMRA and MCF-7 cells were stained green with Cell Tracker Green CMFDA.

Table S1. Separation of cancer cells from blood samples by using different filtration techniques

REF	Medium	Collection efficiency	Purity	Throughput	Cell viability	Release	Culture
5	Whole blood lysed RBC	97%		1×10^6 cells/h		Yes	No
6	Whole blood diluted with EMEM(×8)	>92%		0.4 mL/h		Yes	No
7	Whole blood lysed RBC	90%		1.5 mL/h		No	No
8	Whole blood lysed RBC	~90%		4×10^7 cells/h		Yes	No
9	Whole blood lysed RBC	~90%	>80%	1.5 mL/h		No	No
10	Whole blood diluted with PBS(×10)	~86.5%		120 mL/h	~85%	No	Yes
This work	Whole blood diluted with PBS (×5)	>90%	>80%	2.4 mL/h	>90%	Yes	Yes

References for ESI:

[1] J. Y. Wang, G. D. Sui, V. P. Mocharla, R. J. Lin, M. E. Phelps, H. C. Kolb and H. R. Tseng, *AngewandteChemie-International Edition*, 2006, **45**, 5276-5281.

[2] S. F. Shen, C. Ma, L. Zhao, Y. L. Wang, J. C. Wang, J. Xu, T. B. Li, L. Pang and J. Y. Wang, *Lab on a Chip*, 2014, **14**, 2525-2538.

[3] A. A. S. Bhagat, H. W. Hou, L. D. Li, C. T. Lim and J. Han, *Lab on a Chip*, 2011, **11**, 1870-1878.

[4] J.-S. Park, S.-H.Song and H.-I. Jung, *Lab Chip*, 2009, **9**, 939–948.

[5] B. K. Lin, S. M. McFaul, C. Jin, P. C. Black and H. S. Ma, *Biomicrofluidics*, 2013, **7**.DOI: 10.1063/1.4812688.

[6] T. Huang, C. P. Jia, Y. Jun, W. J. Sun, W. T. Wang, H. L. Zhang, H. Cong, F. X. Jing, H. J. Mao, Q. H. Jin, Z. Zhang, Y. J. Chen, G. Li, G. X. Mao and J. L. Zhao, *Biosensors & Bioelectronics*, 2014, **51**, 213-218.

[7] J. S. Kuo, Y. X. Zhao, P. G. Schiro, L. Y. Ng, D. S. W. Lim, J. P. Shelby and D. T. Chiu, *Lab on a Chip*, 2010, **10**, 837-842.

[8] W. Beattie, X. Qin, L. Wang and H. S. Ma, *Lab on a Chip*, 2014, **14**, 2657-2665.

[9] P. T. Lv, Z. W. Tang, X. J. Liang, M. Z. Guo and R. P. S. Han, *Biomicrofluidics*, 2013, **7**.10.1063/1.4808456.

[10] S. Y. Zheng, H. K. Lin, B. Lu, A. Williams, R. Datar, R. J. Cote and Y. C. Tai, *Biomedical Microdevices*, 2011, **13**, 203-213.

ESI Movies

Movie S1. Red flow was infused into the fluidic channel to simulate the cell infusion and sorting steps (accelerated to 1.5 times the real speed).

Movie S2. Blue flow was infused into the fluidic channel to simulate the cell extraction step (accelerated to 1.5 times the real speed).

Movie S3. The separation of the green fluorescence microshperes in the 10-μm filter matrix (the pore size is 10 μm) were recorded.

Movie S4. The separation of the fluorescence labelled MDA231-LM cells in the 10-μm filter matrix (the pore size is 10 μm) were recorded.

Movie S5. The separation of the MDA231-LM cells from the blood sample in the 10-μm filter matrix (the pore size is 10 μm) were recorded. Time-lapse optical images were acquired, showing separation of MDA231-LM cells.